Supplemental Table 1: Mouse CLIP-seq data.

RBP	Tissue	Binding	Correlation	Source
CELF1	C2C12			Yang et al., 2015
CELF4	Mouse brain	✓		Yang et al., 2015
ELAVL1	Mouse brain			Yang et al., 2015
FUS	Mouse brain; mES neurons	✓	✓	Yang et al., 2015
MBNL1	C2C12			Yang et al., 2015
MBNL1/2	Brain, heart, muscle, C2C12	✓	✓	Yang et al., 2015
MBNL2	Hippocampus	✓	✓	Yang et al., 2015
NOVA1	Mouse brain/cortex	✓	✓	Zhang et al., 2010; Saito et al., 2016
NOVA2	Mouse cortex	✓	✓	Saito et al., 2016
PABPC1	MEL			Yang et al., 2015
PTBP1	C2C12			Yang et al., 2015
PTBP2	Mouse embryonic brain	✓	✓	Licatalosi et al., 2012
RBFOX1	Whole mouse brain	✓	✓	Yang et al., 2015
RBFOX2	mESC; whole mouse brain	✓	✓	Yang et al., 2015
RBFOX3	P19-derived neurons	✓		Yang et al., 2015
RBM3	MEF			Yang et al., 2015
SRRM4	N2A cells			Yang et al., 2015
SRSF1	P19 cells			Müller-McNicoll et al., 2016
SRSF2	P19 cells			Müller-McNicoll et al., 2016
SRSF3	P19 cells	✓	✓	Müller-McNicoll et al., 2016
SRSF4	P19 cells	✓		Müller-McNicoll et al., 2016
SRSF5	P19 cells	✓		Müller-McNicoll et al., 2016
SRSF6	P19 cells	✓	✓	Müller-McNicoll et al., 2016
SRSF7	P19 cells			Müller-McNicoll et al., 2016
TARDBP	Whole mouse brain; mouse brain	✓		Yang et al., 2015
U2AF2	N2A cells; Mouse brain	✓		Yang et al., 2015

Licatalosi DD, Yano M, Fak JJ, Mele A, Grabinski SE, Zhang C, Darnell RB. 2012. Ptbp2 represses adult-specific splicing to regulate the generation of neuronal precursors in the embryonic brain. *Genes Dev* **26**: 1626–1642. doi:10.1101/gad.191338.112

Müller-McNicoll M, Botti V, Jesus Domingues AM de, Brandl H, Schwich OD, Steiner MC, Curk T, Poser I, Zarnack K, Neugebauer KM. 2016. SR proteins are NXF1 adaptors that link alternative RNA processing to mRNA export. *Genes Dev* **30**: 553–566. doi:10.1101/gad.276477.115

Saito Y, Miranda-Rottmann S, Ruggiu M, Park CY, Fak JJ, Zhong R, Duncan JS, Fabella BA, Junge HJ, Chen Z, et al. 2016. NOVA2-mediated RNA regulation is required for axonal pathfinding during development. *eLife* **5**: e14371. doi:10.7554/eLife.14371

Yang YCT, Di C, Hu B, Zhou M, Liu Y, Song N, Li Y, Umetsu J, Lu ZJ. 2015. CLIPdb: a CLIP-seq database for protein-RNA interactions. *BMC Genom* **16**: 51. doi:10.1186/s12864-015-1273-2

Zhang C, Frias MA, Mele A, Ruggiu M, Eom T, Marney CB, Wang H, Licatalosi DD, Fak JJ, Darnell RB. 2010. Integrative modeling defines the Nova splicing-regulatory network and its combinatorial controls. *Science* **329**: 439–443. doi:10.1126/science.1191150

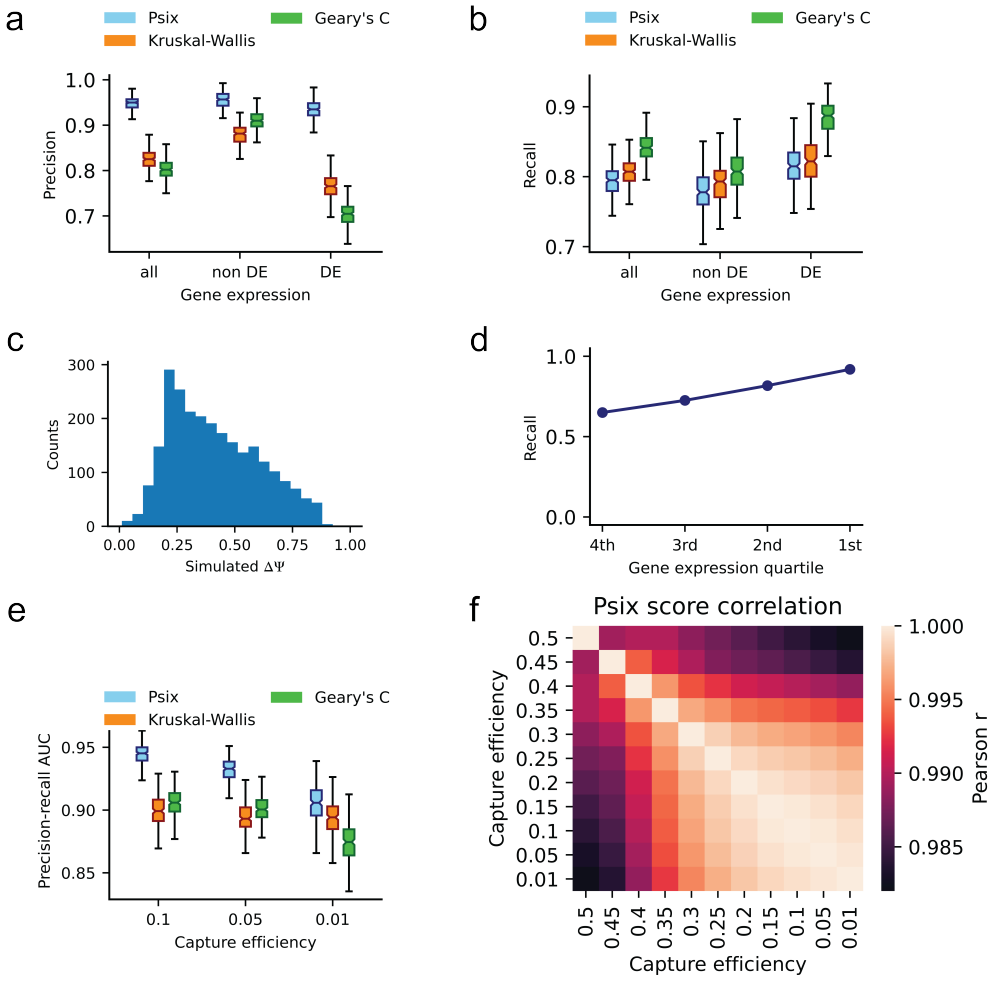

Supplemental Figure 1: a) Precision and b) recall showing success of Psix and other methods at identifying exons simulated to have a $|\Delta\Psi| \geq 0.2$ across a single lineage, in genes simulated as not differentially expressed (non DE), and as differentially expressed (DE). c) Distribution of platonic splicing change in single lineage simulations. Exons simulated without change ($\Delta\Psi = 0$) are not shown. d) Psix recall in the single lineage simulation, in cassette exons sorted into quartiles according to gene expression. e) Area under the precision-recall curve showing success of Psix and other methods at identifying exons simulated to have a $|\Delta\Psi| \geq 0.2$, under three different capture efficiencies, in a single lineage simulation. f) Pearson's correlation of the Psix score in the single lineage simulation using different capture efficiency rates in the model to estimate the probability of each observation.

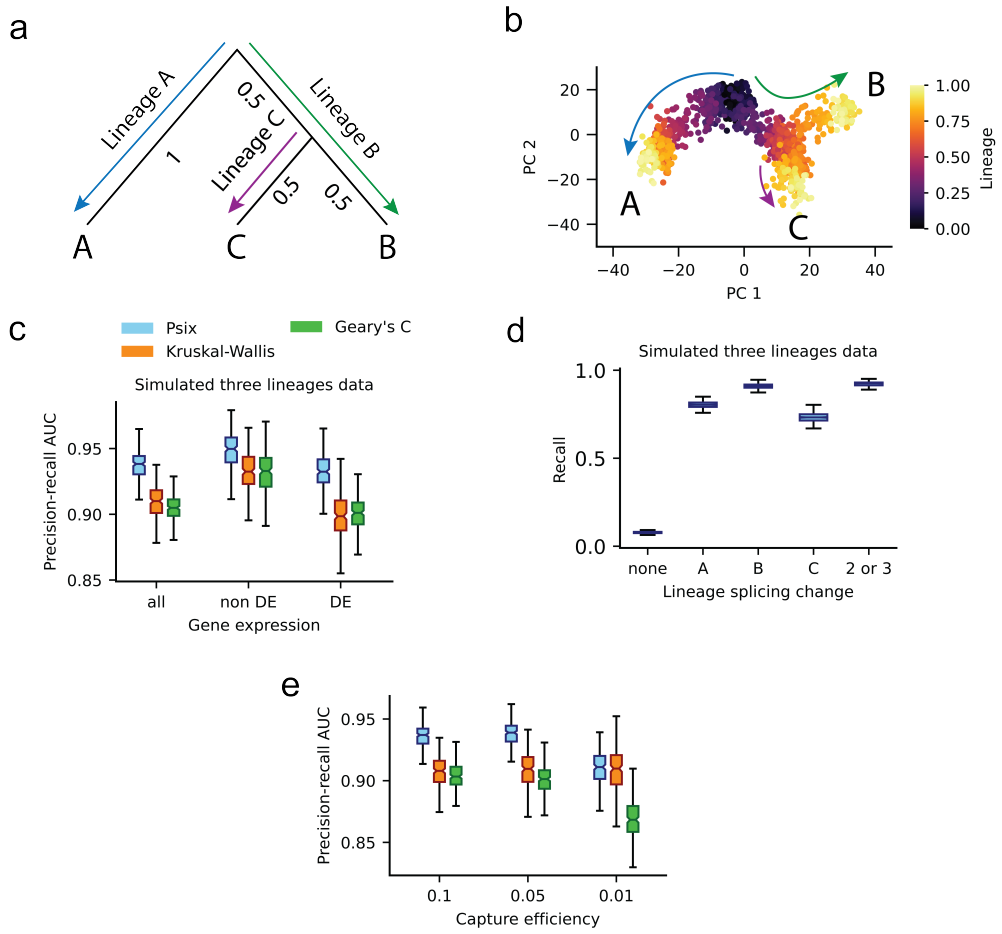

Supplemental Figure 2: a) Simulation of alternative splicing in a complex single-cell population. Phylogenetic tree used as input for SymSim. b) Principal component analysis of the transcriptome landscape of the simulated population. c) Area under the precision-recall curve showing success of Psix and other methods at identifying exons simulated to have a $|\Delta\Psi| \geq 0.2$ across a three lineages, in genes simulated as not differentially expressed (non DE), and as differentially expressed (DE). d) Proportion of exons in the three lineage simulation that are selected by Psix as positive, when they do not change in any branch ("none"), when they only change in one of the three branches, or when they change in two or more branches. e) Area under the precision-recall curve of Psix, the Kruskal-Wallis test, and Geary's C, identifying exons with a $|\Delta\Psi| \geq 0.2$ under different capture efficiencies.

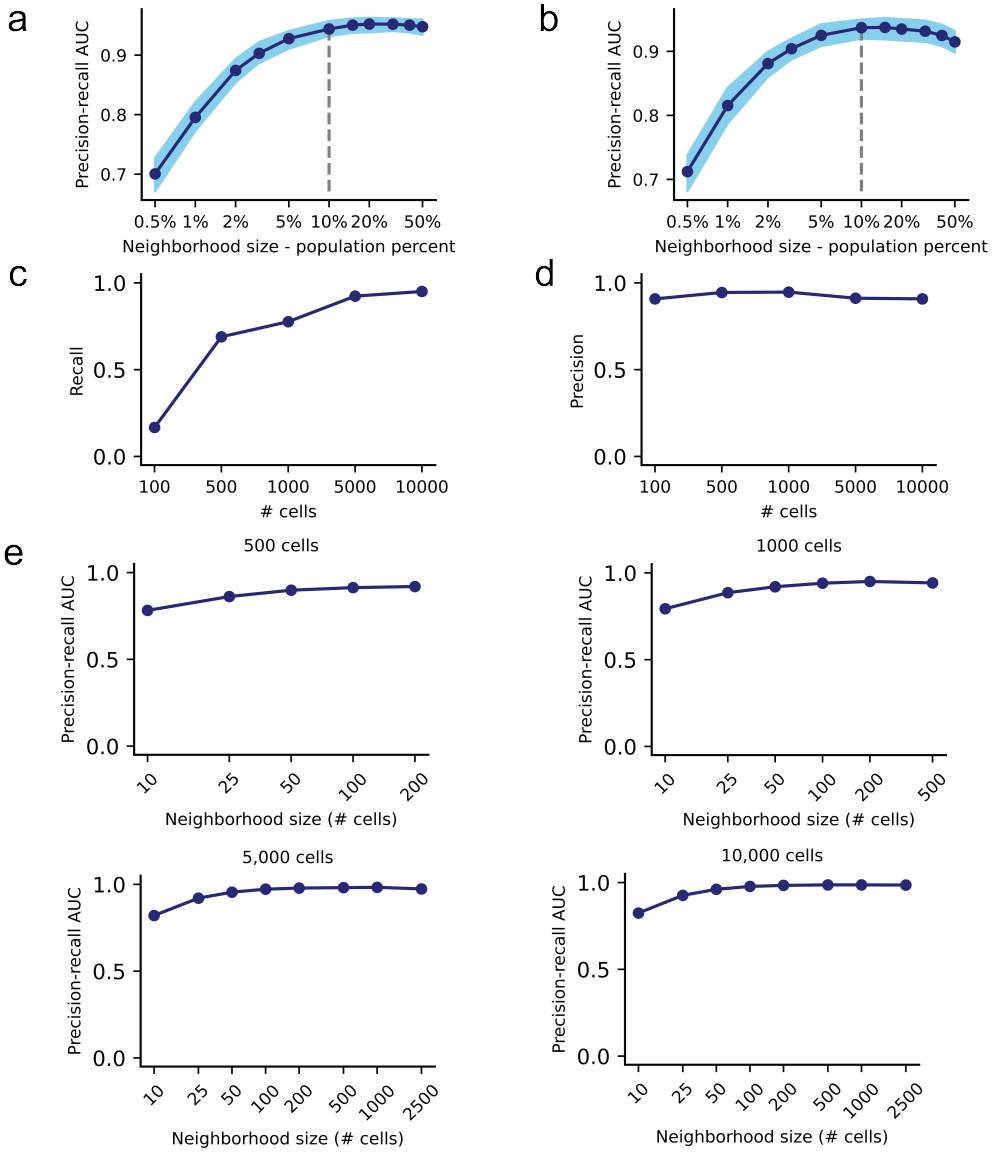

Supplemental Figure 3: a) Effect of neighborhood size on Psix performance in the single lineage simulation. Area under the precision-recall curve of Psix on simulated data with different *k* sizes. Blue area represents 0.05 to 0.95 quantiles. b) Effect of neighborhood size on Psix performance in the three lineages simulation. c) Sensitivity in a single lineage simulation with different numbers of total simulated cells. d) Precision in a single lineage simulation with different numbers of total simulated cells. e) Area under the precision-recall curve dependent in the size of the *k*-neighborhood, in a single lineage simulation with different numbers of total simulated cells.

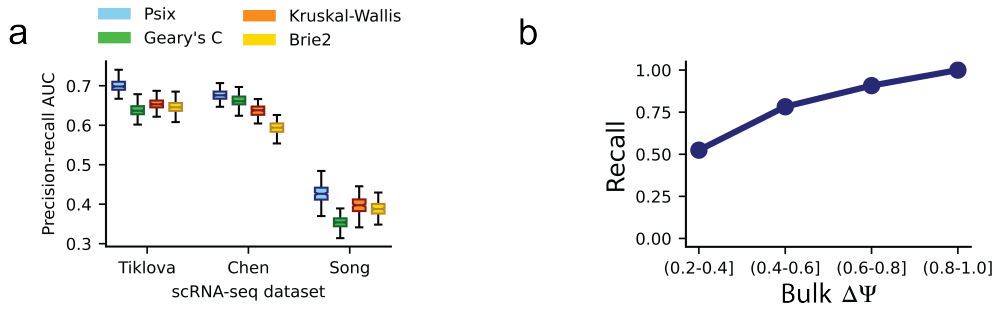

Supplemental Figure 4: a) Area under the precision-recall curve representing the overlap of the exons selected from three real scRNA-seq data with the exons from corresponding bulk datasets. b) Psix sensitivity to detect splicing change is greater for exons with large splicing change in bulk RNA-seq data.

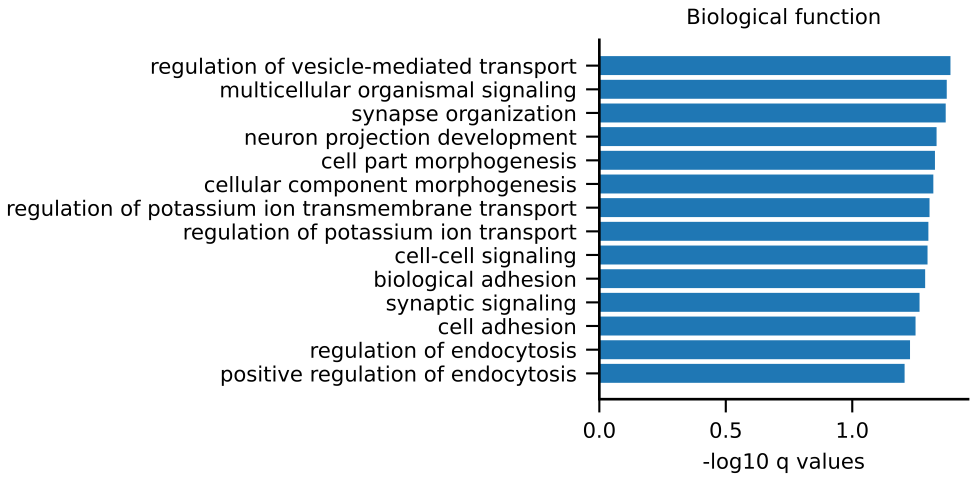

Supplemental Figure 5: Gene Ontology enrichment analysis of the Psix score in the Tiklova dataset (biological function terms).

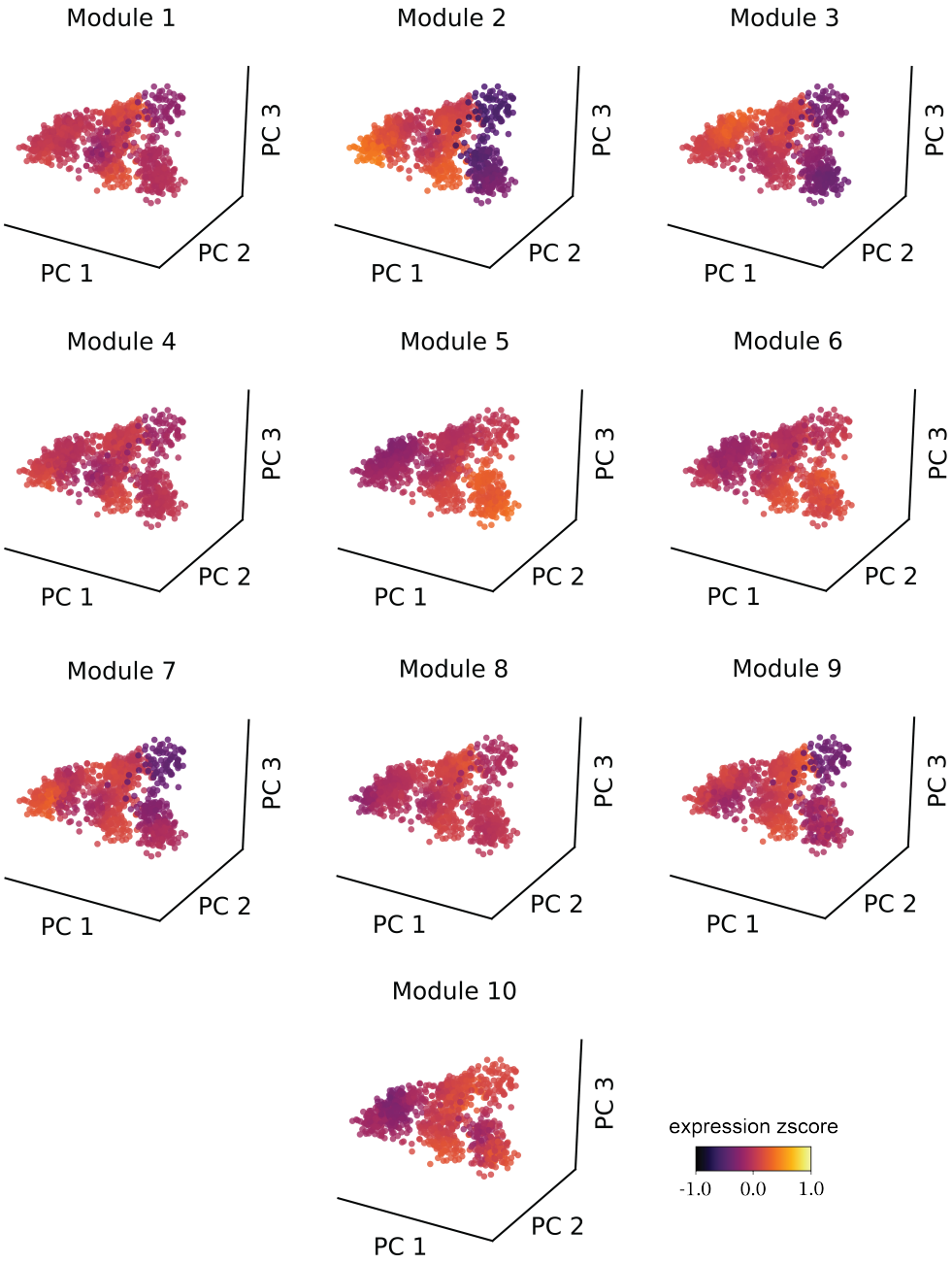

Supplemental Figure 6: Neighbor average zscore of normalized TPM of the genes that contain the cassette exons in each module shown in Figure 3d.

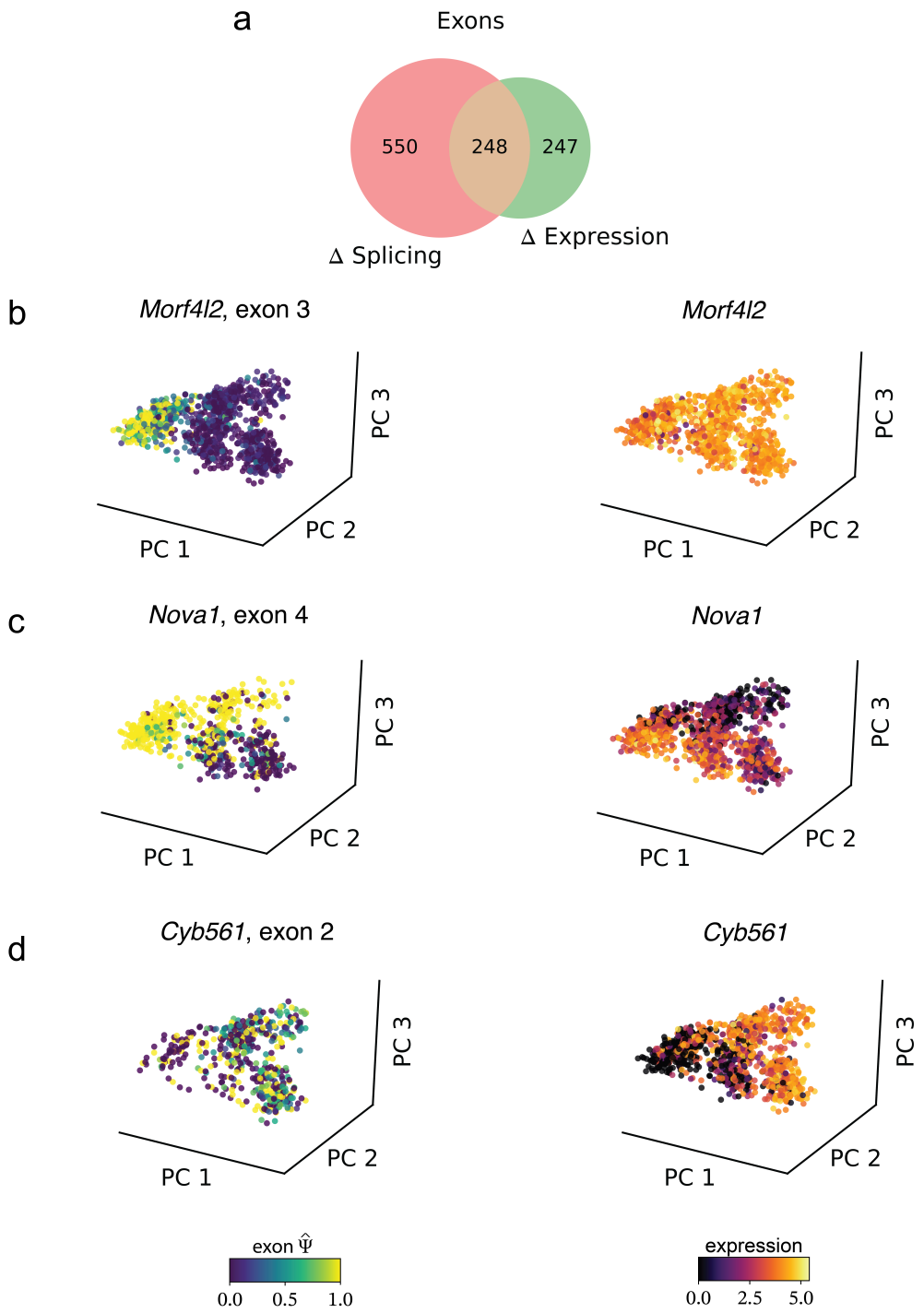

Supplemental Figure 7: a) Venn diagram showing the overlap between cell state–associated cassette exons, and cassette exons in differentially expressed genes in the Tiklova dataset. b) Example of a cell state–associated cassette exon in a gene without differential expression. c) Example of a cell state–associated cassette exon in a gene with differential expression. d) Example of a cell state–independent cassette exon in a gene with differential expression.

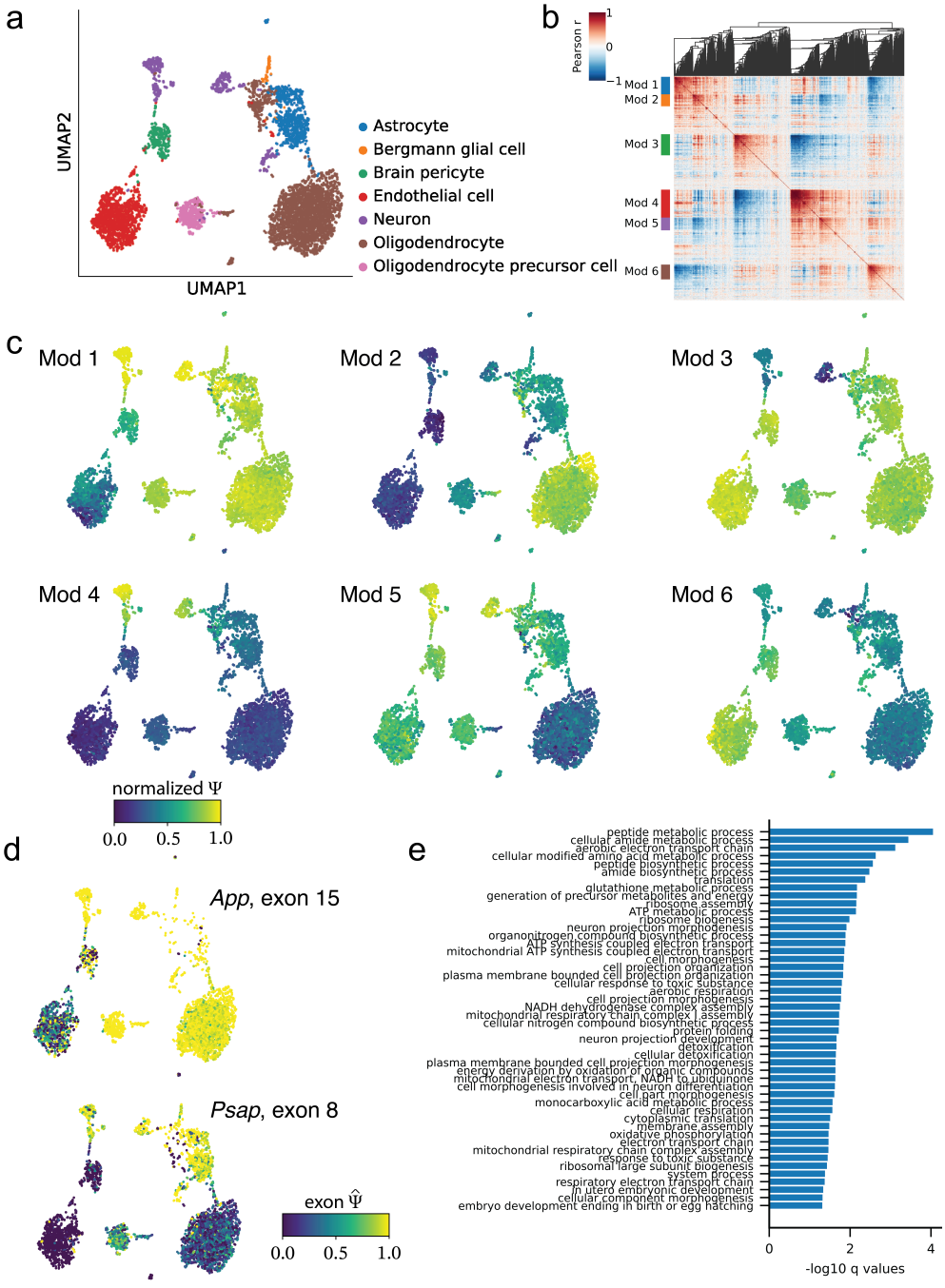

Supplemental Figure 8: a) UMAP of the Brain Neurons subset of the Smart-seq2 *Tabula Muris* dataset. UMAP was applied over the low-dimensional manifold obtained with scVI (Lopez et al. 2018). b) Correlation map of the neighbor average $\overline{\Psi}$ of the cell state–associated exons in the *Tabula Muris* dataset. c) Neighbor average normalized $\overline{\Psi}$ of the exons in each module. d) Examples of some of the top scoring exons. e) Gene Ontology enrichment analysis of the Psix score in the *Tabula Muris* dataset (biological function terms)

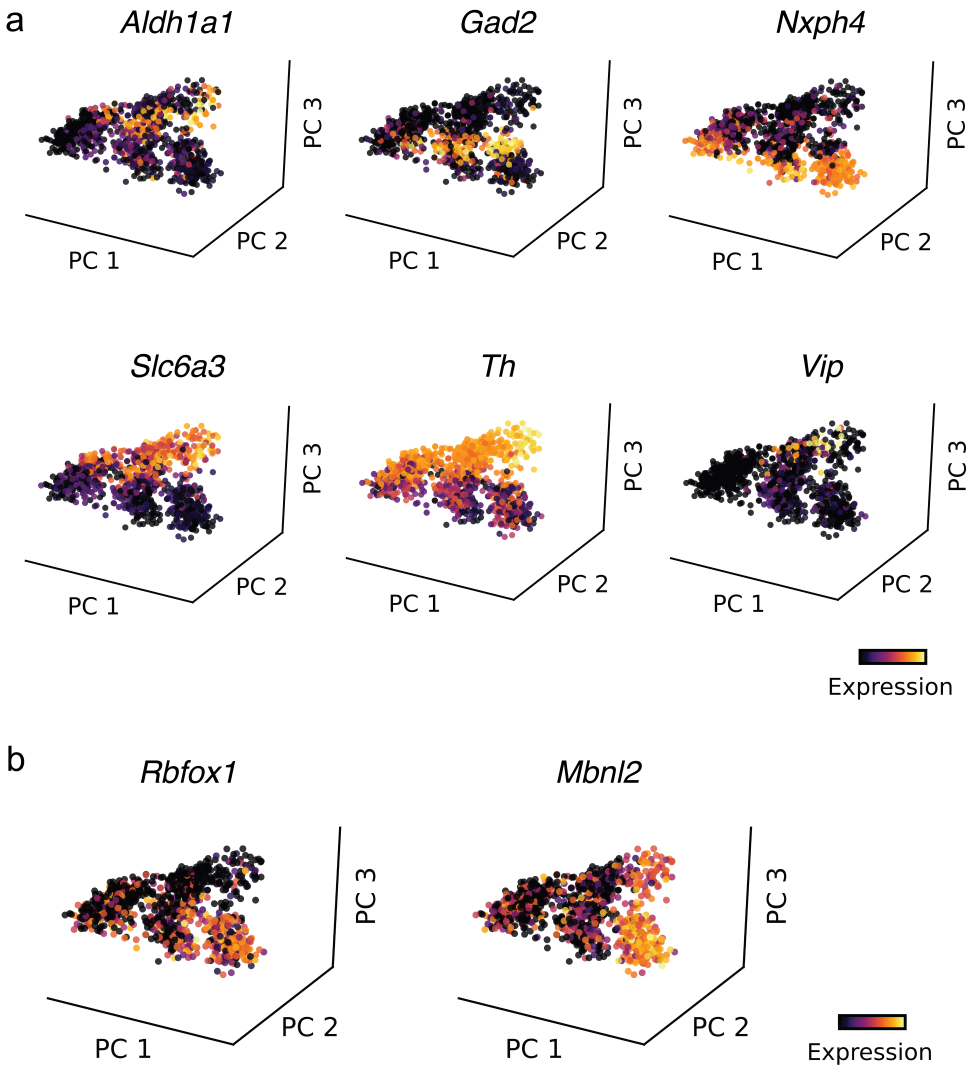

Supplemental Figure 9: a) Principal component 3 is associated with neuron diversity in postnatal day 90 midbrain neurons. Expression of genes characteristic of midbrain neuron subtypes. b) Expression of *Rbfox1* and *Mbnl2* in midbrain dopamine neurons during development.